Crack location in beams using wavelet analysis

Mario Solís[1], Mario Algaba[2], Pedro Galvín[3]

Escuela Técnica Superior de Ingeniería, Universidad de Sevilla

Camino de los Descubrimientos, 41092 Sevilla, Spain

[1]msolis@us.es, [2]marioalgaba@gmail.com, [3]pedrogalvin@us.es

Keywords: damage identification, wavelet analysis, modal analysis, beams

Abstract. This paper applies a methodology for damage detection in beams proposed by the authors. The methodology is based on a continuous wavelet analysis of the difference of mode shapes between a damaged state and a reference state. The wavelet transform is used to detect changes in the mode shapes induced by damage. The wavelet coefficients for each mode are added up and normalized to unity in order to obtain a clear and precise damage assessment. A curve fitting approach reduces the effect of experimental noise in the mode shapes. When only a small number of measuring points are available, a cubic spline interpolation technique provides additional "virtual" measuring points. The interpolation technique may also be used when measuring points are not equally spaced. It also serves as a softening technique of the mode shapes when applied, and no curve fitting approach is used in that case. An antisymmetric extension at both ends of the mode shapes is used to avoid the edge effect in the wavelet transform.

The paper presents the results obtained for steel beams with an induced crack. Several sizes and locations of the crack have been considered. The paper addresses several issues affecting the accuracy of the proposed methodology, such as the number of measuring points and the effect of the extension, curve fitting and interpolation techniques.

Introduction

Wavelet transform appears at the last century like a promising tool in order to treat non-stationary signals [1]. Applications of wavelet transform are diverse: it has been used in biology, metallurgy, finances, internet traffic description, compression and denoise of signals, etc. It is considered that the pioneering application of wavelet transform to detect damage in structures was published in 1994 [2]. Since then, a large number of papers have been devoted to this topic. Wavelet can be applied to time domain as well as space domain functions. Both types of functions have been employed in order to locate defects in different types of structures.

Since wavelet transform is able to detect changes in a signal, it can be used to detect changes in the response of a structure induced by damage. Static deflection and mode shapes of the structure can be used as input space domain signals for wavelet analysis. There are interesting works devoted to the use static deflection to detect damage through wavelet transform [3, 4, 5]. On the other hand, mode shapes analysis has also provided successful results when applied to beams made of aluminium [6], wood [7], composite [8] or pexiglass [9].

Differences of modes shapes have been also used to locate damage in a efficient ad reliable way [10, 11]. Radziensky et al. [12] proposed a hybrid damage detection method for beams, in which wavelet coefficients are combined with other dynamic properties of the structure. They used changes in natural frequencies and modal curvatures to define a damage probability function to weight the wavelet coefficients. The weighting was developed along the beam for each mode shape. In some cases, results for each mode shape were added up.

In this paper, another hybrid damage detection methodology is proposed. It combines changes in natural frequencies with wavelet analysis to enhance the sensibility of wavelet analysis to detect local singularities in the input signal (mode shapes) induced by damage. Preliminary steps of the method consist of processing the input signals in order to reduce effect of experimental noise (curve fitting) and the edge effect (antisymmetric extension). In addition, a cubic spline interpolation technique is performed if the number of measuring points is small or they are not equally spaced. After mode shapes have been processed, a Continuous Wavelet Transform (CWT) of the difference of mode shapes between the damaged and the undamaged structure is performed. The resulting coefficients of the CWT for each mode are added up, but they are weighted according to the change in natural frequencies. Finally, the weighted addition of the coefficients is normalized to unity at each scale for a more clear and efficient damage detection.

Continuous Wavelet Transform. Definitions and properties

The Continuous Wavelet Transform (CWT) of a function f(x) can be defined as:

$$CWT_f(u,s) = \frac{1}{\sqrt{s}} \int_{-\infty}^{+\infty} f(x) \cdot \Psi^*\left(\frac{x-u}{s}\right) \cdot dx \tag{1}$$

Where Ψ^* indicates the complex conjugate of the wavelet function, although it is not always complex. The wavelet function is modified by translation and dilation through translation parameter *u* and scale parameter *s* respectively. The wavelet transform $CWT_f(u, s)$ indicates how similar is the original function f(x) to the wavelet function at a specific location (given by *u*) and for a certain frequency or pseudofrequency (given by scale *s*). The CWT of a numerical (discrete) signal is defined numerically by a set of wavelet coefficients for every location of the original discrete signal and for as many scales as requested. The CWT gives redundant information about the original signal, but it gives more clear information for detecting singularities such as those induced by damage in mode shapes. The Discrete Wavelet Transform avoids redundant information so it is a more efficient algorithm for signal encoding [13], but CWT is more commonly used for damage detection, especially when it is based on space defined signals.

Wavelet functions must fulfill several mathematical requirements in order to be used in wavelet analysis. These mathematical issues are out of the scope of this paper and can be reviewed elsewhere [14]. However, it must be pointed out that the main feature of a wavelet function Ψ is being an oscillatory function with zero average and finite length (compact support),

$$\int_{-\infty}^{\infty} \Psi(x)dx = 0 \tag{2}$$

Another important feature of the wavelet function is the number of vanishing moments. If a wavelet function has N vanishing moments, then:

$$\int_{-\infty}^{\infty} x^k \Psi(x)dx = 0 \quad for \;\; k=0....N-1 \tag{3}$$

For any polynomial of smaller order than the number of vanishing moments, the wavelet transform gives null values. Therefore, the number of vanishing moments indicates how sensitive is the wavelet to low order signals, and it can be chosen so as to take only into account the components of the signal above certain order value.

In this paper, the well-known Daubechies [15] wavelet family with 2 vanishing moments has been used. For the beams analysed in this paper, a higher number of vanishing moments proved to be less sensitive to damage. That may suggest that the effect of damage induces a change of order 2 in mode shapes that should not be neglected. A number of 2 vanishing moments indicates that the wavelet is sensitive to the second derivatives of the mode shapes, and therefore to modal curvatures. Thus, the wavelet analysis will give information about changes in modal curvatures, which are well known as a sensitive damage detection parameter.

Damage detection methodology

This section describes the proposed hybrid damage detection methodology in beams. The first step is to obtain modal parameters from the structure. Once mode shapes are available, they must be numerically processed in order to make them useful input signals for wavelet analysis.

The first numerical treatment consists of an antisymetric extension of the mode shapes in order to avoid the so called edge effect of wavelet transform. This is an undesirable phenomenon related to the mathematical definition of the wavelet definition. Wavelet transform is defined as an infinite integral transform whereas the input signal has finite length. Thus, wavelet transform shows a singular behaviour at both ends of the input signal. This leads to high peaks in the wavelet coefficients which may mask the damage effect. By extending the original signal, the edge effect is moved to the ends of the extended signal, and the original length is not affected by this phenomenon. The antisymetric extension provides a good continuity at both ends of the original signal to avoid singularities in those areas.

The second numerical treatment deals with reduction of experimental noise effect in mode shapes. For this goal, a curve fitting approach is proposed. This softening technique is implemented by using 'mslowess' built-in function of MatLab software [16]. It consists of a weighted quadratic least squares approach performed at every location of the original mode shape considering a span of ten neighbouring points centered at that location.

When only a small number of measuring points is available, an interpolation process is included to obtain new "virtual" measuring points to the input signal of the wavelet analysis, since it requires a significant number of components as an input to obtain meaningful results. For this purpose, a cubic spline interpolation technique is introduced [6, 9, 12]. If the original measuring points are not equally spaced, the interpolation process can also be used to obtain equally spaced "virtual" measuring points, which is a requirement for the input signal of wavelet transform. For instance, it can be useful if there are noisy measuring points that must be disregarded. Moreover, the interpolation process smoothes the mode shape by itself, so the previously described smoothing technique through curve fitting is not necessary when interpolation is applied.

Once the extended and smoothed mode shapes have been obtained, the wavelet analysis is applied.

Firstly, the extended difference of mode shapes ($\Phi_{diff,ext}$) is computed from the difference between the smoothed extended damaged ($\Phi_{s,ext,d}$) and undamaged ($\Phi_{s,ext,u}$) mode shapes.

$$\Phi_{diff,ext} = (\Phi_{s,ext,d} - \Phi_{s,ext,u}) \tag{4}$$

A CWT of each extended mode shape difference is done to give information about changes in mode shapes. The CWT for the ith mode shape can be written as:

$$CWT^{i}_{\Phi_{diff,ext}}(u,s) = \frac{1}{\sqrt{s}} \int_{-\infty}^{+\infty} \Phi^{i}_{diff,ext}(x)\, \Psi^{*}\left(\frac{x-u}{s}\right) \cdot dx \tag{5}$$

At this point, only the CWT coefficients that corresponds to the original signal, and therefore to the real structure, are considered. The coefficients corresponding to the antisymmetric extension of the signal at both ends are disregarded.

In order to simplify the analysis of the CWT for each mode shape and to draw an overall result for damage detection, the absolute values of CWT coefficients of each mode shape are added up to obtain a global wavelet parameter for damage detection CWT_{sum}. This global parameter may also reduce the effect of noise that is present in a specific mode shape, whereas it will always accumulate the effect of damage for all mode shapes.

In addition, the coefficients for each mode shape are weighted according to its corresponding change in natural frequencies. It is assumed that those modes that exhibit a higher frequency change are more sensitive to damage and therefore changes in those mode shapes are more significant, whereas the mode shapes that do not change their natural frequencies are almost disregarded. The weighted addition of the coefficients can be written as:

$$CWT_{sum}(u,s) = \sum_{i=1}^{N} CWT^{i}_{\phi_{diff}}(u,s) \cdot (1 - \frac{\omega_u^i}{\omega_d^i})^2 \tag{6}$$

where ω_u^i and ω_d^i stand for the experimentally identified natural frequencies of mode shape i for the undamaged and the damaged state respectively. Finally, this paper proposes a normalization of the coefficients for each scale so maximum value is unity for every scale ($CWT_{NORM}(u,s)$). It is expected that the perturbation in the mode shape induced by damage leads to high values (around unity) for all scales, since damage is supposed to produce higher wavelet coefficients for higher scales at damage location whereas noise is likely to produce local peaks at certain scales and not to produce such a trend [5, 9].

$$CWT_{NORM}(u,s) = \left. \frac{CWT_{sum}(u,s)}{\max[CWT_{sum}(u,s)]} \right|_{s} \tag{7}$$

Experimental test

Five steel I-beams have been tested to apply the proposed methodology. The beams of length L=1280 mm, height h=100 mm, width b=50 mm, web thickness h_w=4.5 mm, flange thickness h_f=6.8 mm and mass per unit length m=8.1 kg/m have been damaged by a saw cut. The cuts are 1 mm width approximately. Table 1 describes the different damage scenarios.

Table 1: Damage scenarios.

Scenario	0	1	2	3	4
Cutting location	Undamaged	0.5L	0.5L	0.25L	0.25L
Cup depth		30 mm	20 mm	30 mm	20 mm

The experimental program involved dynamic characterization of the specimens by modal analysis. An impact force was applied at one end of the beams by an instrumented impact hammer, and the response was measured at 65 points distributed along the beam every d=20mm using piezoelectric accelerometers. The beams were hung in two soft springs at both ends with ks=145.8 N/m stiffness, approaching a free-free boundary condition (Fig. 1). Eleven accelerometers were distributed in seven experimental set ups to eventually obtain 65 measuring points. The reference signal for the set ups was the applied impact force. For each set-up, several impacts were performed in order to eventually obtain average values and reduce the experimental noise effect. Impact response was acquired in 30 seconds per channel per set-up. The data were sampled to 16384 Hz.

The wavelet based damage detection methodology has been applied using only the first three vertical bending mode shapes of the beams. presents the three natural frequencies that have been identified for each damage scenario (first values) with the Modal Assurance Criteria values (MAC) obtained between each damaged mode and the corresponding undamaged one, respectively.

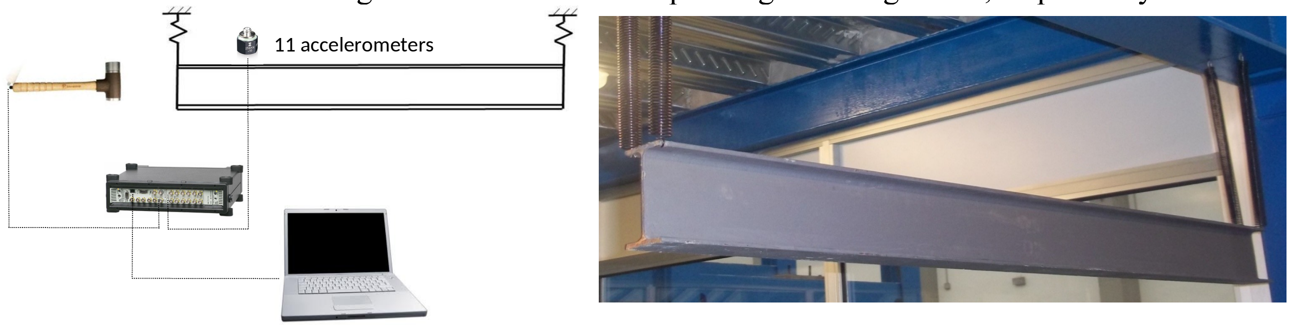

(a) (b)

Fig. 1 (a) Experimental configuration and (b) test set-up in the laboratory.

Table 2: Experimental natural frequencies (Hz) for each damage scenario / MAC values for each mode compared to the reference state.

Mode\Scenario	0	1	2	3	4
1	415.65	300.96 / 0.99258	362.28 / 0.99795	364.75 / 0.96874	397.27 / 0.99413
2	1032.7	1027.35 / 0.99874	1030.15 / 0.99829	822.99 / 0.89465	932.71 / 0.96742
3	1786.75	1473.96 / 0.93651	1634.17 / 0.98433	1557.21 / 0.84222	1663.19 / 0.95711

Natural frequencies and MAC values decrease as the damage is more severe. Nevertheless, MAC values are always close to one, indicating that mode shapes are similar to those obtained for the undamaged state.

Results

Fig. 2 shows the results obtained when applying the proposed methodology to the tested beams. It also shows the influence of the numerical treatments of mode shapes in the results. They show the normalized coefficients along the beam (horizontal axis of each figure) for different scales (vertical axis of each figure). Results for scenarios 1 to 4 are shown in rows of figures 1 to 4 respectively in fig. 2. Figs. 2.a shows the results if no extension and no softening technique is applied to mode shapes. Figs. 2.b show the results when applying the antisymmetric extension. Figs. 2.c show the results when applying also the softening technique. Finally, figs. 2.d shows the results when considering only 13 out of the original 65 measuring points.

Figs. 2 (a) shows that when no extension is applied, the edge effect produces high peaks at the ends of the beam which mask any other information along the beam. Figs. 2(b) show that the extension of the mode shapes makes disappear the edge effect. Thus, the proposed antisymmetric extension is reliable and efficient for the proposed goal. However, experimental noise is still present in the mode shapes and no clear damage location is obtained. High values are obtained at 0.5L for damage scenarios 1 and 2 and at 0.25L for scenarios 3 and 4, but some noisy and confusing values are present in the results. Finally, when the softening technique is applied (Figs. 2 (c)) damage detection and location is clear for all the scenarios. No presence of experimental noise or edge effect is observed in the results, so existence and location of damage is clear. It can be observed that highest values are obtained at damage location for all the scales.

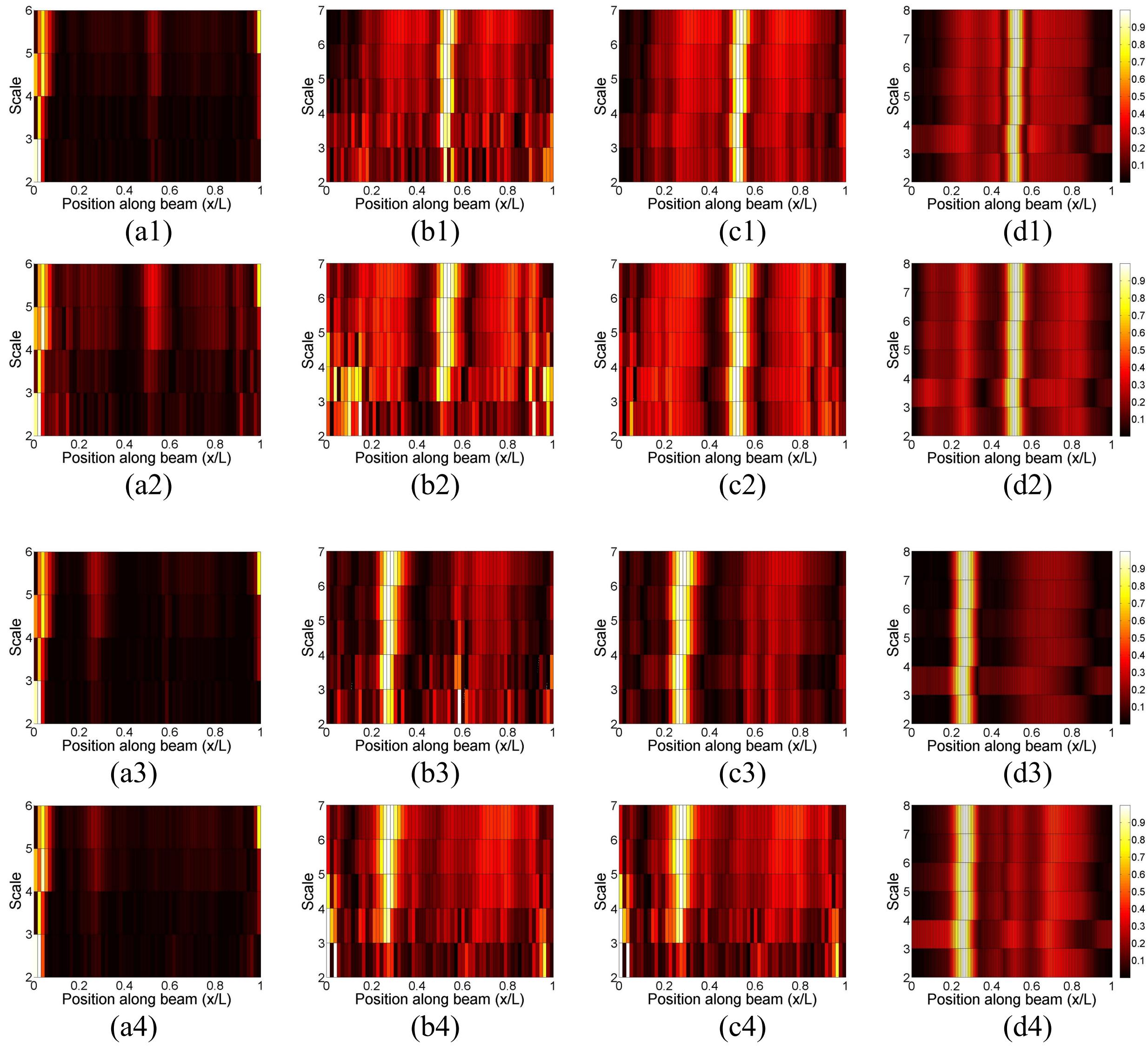

Fig. 2 Resulting wavelet coefficients for damage scenario 1 (row 1), damaged scenario 2 (row 2), damaged scenario 3 (row 3) and damaged scenario 4 (row 4). (a1:a4) without any numerical process of mode shapes, (b1:b4) with extension, (c1:c4) with extension and softening technique (d1:d4) with 13 measuring points and interpolation.

Figs. 2(d) show that when only 13 measuring points are considered and the interpolation technique is employed, the results are almost as clear as with 65 measuring points. This number of measuring points (13) is considered as a threshold value by the authors for this application, after trying with different values.

If no normalization of wavelet coefficients is applied, then singular behavior of wavelet coefficients at damage location is more significant with higher scales, reaching the highest values for the highest scale [17]. The higher the values, the more clear is the damage effect. Indeed, higher values are obtained as damage is more severe. Fig. 3 shows the maximum values of wavelet coefficients obtained for all the damage scenarios considered for 13 to 23 uniformly distributed sensors. The trend for all figures indicates that damage is more clearly detected as the number of measuring points increase. However, there are some fluctuations that can be explained by the location of sensors.

When one sensor is located exactly at the damage position, a higher maximum value of wavelet coefficients is obtained. When damage is located at L/2, a sensor is located at that position when the number of uniformly distributed sensors is odd, and values for odd number of sensors is higher than those obtained for even numbers (Fig. 3(a) and 3(b)).

When damage is located at L/4, a sensor i is located at that position if $i \cdot L/(n-1) = L/4$, being i an integer number (ith position of sensor) and n the total number of sensors. For the range of number of measuring points considered in Fig. 3, this condition takes place for $n=13$, $n=17$ and $n=21$. It an be observed in Figs. 3(c) and 3(d) that local maximum of values of wavelet coefficients are obtained for those numbers (there is only an exception for a local maximun for 18 points in Fig. 3(c))

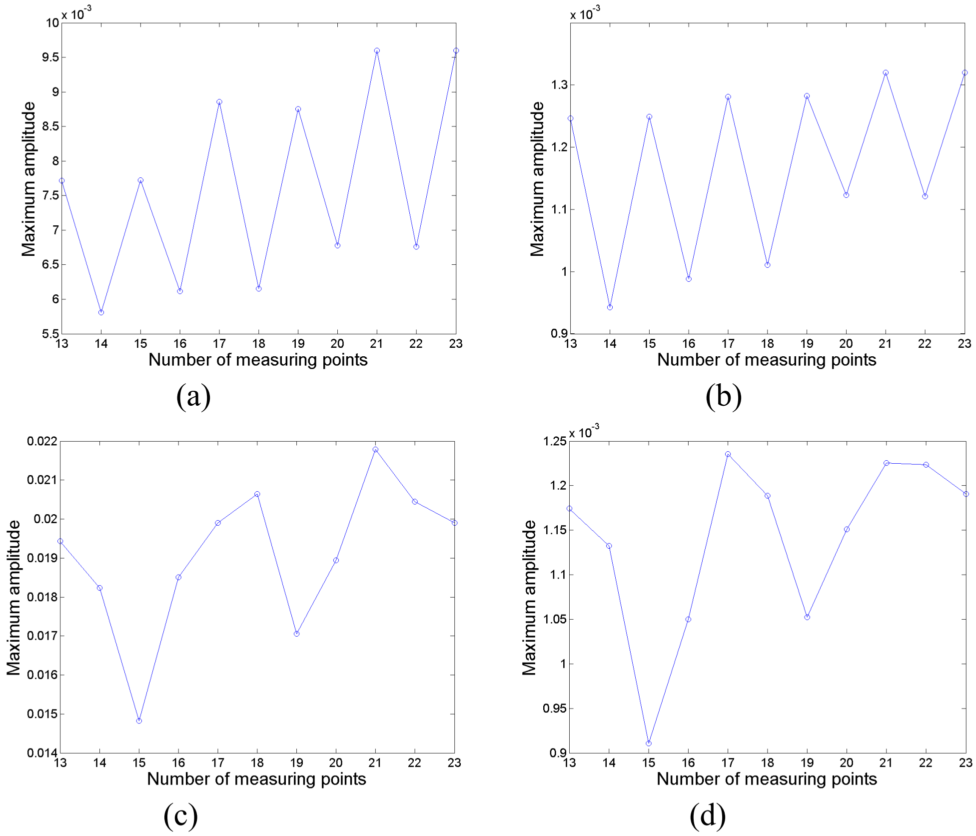

Fig. 3 Relation between initial number of measuring points and the maximum wavelet coefficients amplitude for scenarios 1(a), 2(b), 3(c) and 4(d)

Conclusions

The paper presents a combined modal-wavelet analysis for crack location in steel. The method is based on the wavelet analysis of the difference of mode shape vectors between a damaged and a reference state. The absolute wavelet coefficients values for each mode are added up creating a global damage index. For the addition, the coefficients are weighted according to the change in natural frequencies between the damaged and the reference state. Finally, coefficients are normalized for each scale so more information can be obtained from the analysis of every scale in just one picture and damage location is more clear and precise.

The proposed treatments for avoiding the wavelet edge effect and the experimental noise have proven to be effective. The suggested methodology is simple and easy to use and it is sensitive to crack depths of 20% of the height of the beam when using only 13 measuring points and 3 experimentally identified mode shapes. Future research will explore the sensitivity of the methodology with different crack depths, measuring points and number of modes.

Regarding sensor distribution and location, the paper also proves that more clear results are obtained if a sensor is located at damage location.

Acknowledgments

This research was funded by the Spanish Ministry of Science and Innovation (*Ministerio de Ciencia e Innovación*) through research project BIA2010-14843. Financial support is gratefully acknowledged.

References

[1] A. Haar, Zur Theorie der orthogonalen Funktionensysteme, Mathematische Annalen. 69 331-371. (1910).

[2] C. Surace, R. Ruotolo, Crack detection of a beam using the wavelet transform, Proceedings of the 12th International Modal Analysis Conference (1994) 1141-1147.

[3] K.M. Liew, Q. Wang, Application of wavelet theory for crack identification in structures, Eng. Mech.-ASCE 124 (2) (1998) 152-157.

[4] Q. Wang, X. Deng, Damage detection with spatial wavelets, Int. J. Solids Struct, 36 (23) (1999) 3443-3468.

[5] M. Rucka, K. Wilde, Crack identification using wavelets on experimental static deflection profiles, Eng.Struct. 28 (2006) 279-288.

[6] S. Zhong, S. O. Oyadiji, Crack detection in simply supported beams without baseline modal parameters by stationary wavelet transform, Mech. Syst. Signal Pr 21 (2007) 1853-1884.

[7] Ch. Hu, M. Afzal, A wavelet analysis-based approach for damage localization in wood beams, Journal of Wood Science. 52 (2006) 456-460.

[8] Z. Wei, L. Yam, L. Cheng, Detection of internal delamination in multi-layer composites using wavelet packets combined with modal parameter analysis, Composite Structures 64 (2004) 377-387.

[9] M. Rucka, K. Wilde, Application of continuous wavelet transform in vibration based damage detection method for beams and plates, J. Sound Vib. 297 (3-5) (2006) 536-550.

[10] U. P. Poudel, G. Fu, J. Ye, Wavelet transformation of mode shape difference function for structural damage location identification, Earth. Eng. Struct. Dyn. 36 (8) (2007) 1089-1107.

[11] U. P. Poudel, G. Fu, J. Ye, Structural damage detection using digital video imaging technique and wavelet transformation, J. Sound Vib. 286 (4-5) (2005) 869-895.

[12] M. Radzieński, M. Krawczuk, M. Palacz, Improvement of damage detection methods based on experimental modal parameters, Mech. Syst. Signal Pr. 25 (2011) 2169-2190.

[13] S. Mallat, A Wavelet Tour of Signal Processing, Academic Press, London, 1999.

[14] G. Strang, N. Truong, Wavelets and Filter Banks, Wellesley College Press, Cambridge, 1996

[15] I. Daubechies, Orthonormal bases of compactly supported wavelets, Comm. Pure Appl. Math. 41 (7) (1988) 909-996.

[16] T. Mathworks, Matlab (2011).

[17] M. Algaba, M. Solís, P. Galvín, Wavelet based mode shape analysis for damage detection Proceedings of the 30th International Modal Analysis Conference (2012) 1141-1147.